The first luminescence dating of Tibetan glacier basal sediment

Zhu Zhang, Shugui Hou, Shuangwen Yi

School of Geographic and Oceanographic Sciences, Nanjing University, Nanjing, 210093, China

Correspondence to: Shugui Hou (shugui@nju.edu.cn)

5   **Abstract.** Dating of ice cores drilled in the high mountain glaciers is difficult because seasonal variations cannot be traced at depth due to rapid thinning of the ice layers. Here we provide the first luminescence dating of the basal sediment of the Chongce ice cap in the northwest Tibetan Plateau. Assuming the sediment is of similar (or older) age as the surrounding ice, the luminescence dating of 42 ± 4 ka provides an upper limit for the age of the bottom ice at the drilling site. This result is more than one order of magnitude younger than the previously suggested age of

10   the basal ice of the nearby Guliya ice cap (~40 km in distance).

1 Introduction

Ice cores from the high elevation regions provide a wealth of information for past climatic and environmental conditions that extends beyond the instrumental period. A precise chronology is the essential first step for a reliable

15   interpretation of the ice core records. The Tibetan Plateau (TP), sometimes called "the Roof of the World", is the world's highest and largest plateau with an average elevation exceeding 4000 m above sea level (a.s.l.) and an area of 2.5 Million square kilometers. It has the largest number of glaciers outside the polar regions. In 1992, a 308.6 m ice core to bedrock was recovered from the Guliya ice cap on the northwest TP (Fig. 1). Top 266 m of the core was dated to a period spanning 110 ka, and the ice below 290 m was suggested to be more than 500 ka old due to ^{36}Cl-

20   dead in the ice (Thompson et al., 1997). This makes it the second oldest continuous ice core, only younger than the Antarctic EPICA Dome C ice core. During the past two decades, the Guliya ice core record has been widely used as a benchmark for correlating regional climate variables in the Westerlies region of the central Asia and the northern Tibetan Plateau. However, Cheng et al. (2012) suggested a substantial revision of the Guliya chronology due to the enormous inconsistence between the δ^{18}O records of the Guliya ice core and the Kesang stalagmite (Fig. 1 and

25   Supplement).

Luminescence dating can be readily applied to most terrestrial sediments and can be used to date sediments on timescales from 10^1 to 10^5 years, encompassing the entire late Quaternary (Fuchs and Owen, 2008). Dating errors within a few percent of the age can be achieved depending upon the nature of the sediment and the laboratory

methods. During the recent decades, optically stimulated luminescence (OSL) method has been successfully used for dating glacial sediments on the TP and surrounding regions (e.g., Owen et al., 2003; Ou et al., 2014; Hu et al., 2015). Willerslev et al. (2007) provided the first luminescence measurements on the single grains of quartz and feldspar extracted from a sample cut out of an opaque part of the Greenland Dye 3 basal ice containing dispersed sandy and silty particles. To our knowledge, this is the only published luminescence dating of glacier basal ice so far. As pointed out by the authors, at the time when the Dye 3 ice core was drilled (1979–1981), no standard apparatus or procedures were used to avoid inadvertent exposure to light during the drilling and subsequent handling, inspection and storage of the ice cores. For this reason, the sample may be considered to be highly problematic for luminescence dating (Willerslev et al., 2007).

2 The Chongce ice cores

In 2012, we drilled two ice cores to the bottom with the length of 133.8 m and 135.8 m respectively, and a shallow ice core with length of 58.8 m at an altitude of 6010 m a.s.l. from the Chongce ice cap (Fig. S1). The Chongce ice cap is located in the west Kunlun Mountains on the northwest TP, with a snowline altitude about 5900 m a.s.l.. It is 28.7 km in length, covering an area of 163.06 km^2, with a volume of 38.16 km^3. The measured ice temperature is about -8.8 °C at depth of 130 m for both the 133.8 m and 135.8 m core boreholes. The drilling sites are about 40 km away from the Guliya drilling site (Fig. 1). The very bottom of the core is a combination of sediment and ice (see picture in Fig. S1). No special precautions were taken to avoid exposure to light during the drilling operation. Therefore, in 2013, two more ice cores to the bottom were recovered with the length of 216.6 m and 208.6 m respectively at an altitude of 6100 m a.s.l. (35°14'57" N, 81°5'28" E. Fig. S1). This time we paid special attention to avoid exposure to light during the drilling and subsequent procedures. The drilling was performed at night. When it was close to the bottom, the cores, together with chips, were recovered in faint red light. They were directly sacked into opaque plastic bags and immediately wrapped with aluminium foil and adhesive tape. The ice cores were kept frozen and transported to the cold room in the Nanjing University for further processing.

3 Sample preparation and measurements

Sample preparation was performed under the safe red light in the Luminescence Dating Laboratory of the Nanjing University. The total bottom sediment including ice is 1431.7 g. We first took a small portion of the sediment (13.4 g) for measuring ice content, which is determined by weighting the mass before and after drying, resulting in ~30%

2

ice (water equivalent) content. As the water content may have varied over the entire burial period of the sample, we assigned a relative uncertainty of 50% to allow for possible fluctuations. Afterwards, this part of sediment was dried in oven (<60 °C). About 5 g dried sediment was ground to fine powder for determining U, Th and K concentrations by neutron activation analysis (NAA) at the China Institute of Atomic Energy, Beijing. The results

5   are given in Table 1. As the measured concentrations are normally low, the accuracy of the dose rates, calculated from the NAA results, may have been affected by the inhomogeneity of the deposits. Therefore, ~ 100g sample was also measured for >24 h using the high-resolution gamma spectrometry (Table S1). The sample was ignited at 450 °C, cast in wax and stored for >3 weeks to assure equilibrium conditions for ^{226}Ra – ^{222}Rn decay (Murray et al., 1987).

10   The rest of the sediment (~1300 g) was put into a beaker and melted in the Luminescence Dating Laboratory at room temperature (~ 20 °C). The melt water was carefully extravasated. This process was repeated to leave as little water inside the beaker as possible. Then the sediment was filtered through the 200 μm wet sieve. The filtered sediment was successively soaked in the 10% hydrochloric acid and 30% hydrogen peroxide to remove carbonate and organic matters. Afterwards, the residual was wet-sieved to separate the coarse grains (90 - 150 μm) from the

15   fine grains (<40 μm).

The coarse grains were then separated by dense liquid (2.58 g.cm^{-3}), resulting in the coarse quartz grains at the bottom. After purified with deionized water, the coarse (90 - 150 μm) quartz grains were immersed in 40% hydrofluoric acid for 40 minutes to remove any remaining feldspar contamination, and in 10% hydrochloric acid for 40 minutes to remove residual fluoride. The purity of the quartz was determined using the OSL-IR depletion ratio

20   method (Duller, 2003). Even after being etched (40% HF, 40 minutes) twice, it was not possible to remove feldspar completely. So, a post-IR measurement with blue LED stimulation (Banerjee et al., 2001) was applied to the coarse grain quartz measurements.

As for the fine grains (<40 μm), a fraction (4 - 11 μm) was further isolated according to 'Stocks' law. To extract pure fine quartz grains, the sample was submerged first in the 40% fluosilicic acid for 10 days, and then in the 10%

25   hydrochloric acid to remove any fluorides. The purity of treated fine grains was checked by the same method as that used with the coarse grains quartz (Duller, 2003). Samples with IRSL (infrared stimulated luminescence) vs. blue OSL signal ratios over 10% of unity would be re-treated with fluosilicic acid until the ratio was within 10% of unity. The coarse quartz grains (90 - 150 μm) were then mounted on stainless steel discs (~2 mm in diameter) using the Silkospray silicone oil, and the fine quartz grains (4 - 11 μm) were settled on discs using pure water with a

30   pipette. Measurements were performed on a Risø TL/OSL reader (model DA-20C/D), fitted with blue LEDs (470 nm, ~80 mW.cm^{-2}), infrared LEDs (870 nm, ~135 mW.cm^{-2}) and a ^{90}Sr/^{90}Y beta source (Bøtter-Jensen et al., 2010).

The OSL signal from the quartz grains was detected by a 9235QA photomultiplier tube through a 7.5 mm Schott U-340 detection filter.

The quartz equivalent doses (D_e) were determined using the single aliquot regeneration (SAR) protocol (Murray and Wintle, 2000). A preheat temperature of 260 °C with a cuteat of 220 °C was selected for De measurement with an elevated temperature (280 ˚C) blue light bleach at the end of each cycle. The early background subtraction (first 0.16 s minus background from 0.16 - 0.32 s interval) was used for signal integration, and to minimize the influence of slow and medium components (Cunningham and Wallinga, 2010).

Individual D_e values were obtained using a single-saturating exponential fitted in Analyst version 4.31.7 (Duller, 2015). The uncertainty of individual D_e values was calculated using counting statistics and an instrumental uncertainty of 1.5%.

4 Results and discussion

The basic assumption of the OSL dating technique is that the mineral grains were fully bleached before deposited. The possibility of complete bleaching of the grains decreases for materials from supraglacial debris, to englacial debris, to basal debris (Fuchs and Owen, 2008), suggesting that extreme care should be taken when applying the luminescence dating techniques to basal debris. The OSL dose-response and decay curves of the quartz aliquots are shown in Fig. 2. It's apparent that parts of the coarse grain (90 - 150 μm) quartz aliquots approach the saturated level, but all the fine grain aliquots are similar and well below the saturated level. The decay curves of the fine grain (4 - 11 μm) show that the OSL signal decreases very quickly and approaches to background level during the first seconds of stimulation. We further decomposed the natural OSL signal of the fine grain aliquots into fast, medium and slow components (Fig. S2). Fast component accounts for around 87% of the natural signal, indicating that the signal is fast component dominant. However, the OSL decay curves of the coarse grain aliquots display a relatively slow trend (Fig. 2). We also performed scanning electron microscope of the sediment sample. A typical coarse grain quartz is shown in Fig. S3. Its angular texture and low degree of deformation suggest that this coarse grain quartz might have been scoured from bedrock, which mainly consists of Triassic high-K granitoids in the west Kunlun Mountains (Wang et al., 2013). In addition, the D_e distribution presented in Fig. 3 shows a narrow and nearly symmetric shape for the fine quartz grains, indicating sufficient bleaching of the fine quartz grains. Based on these results, we believe that only the fine grain quartz is appropriate for luminescence dating of our sample, hence excluded the coarse grain quartz from further calculation. The same conclusion was also reached in some previous studies on Himalayan glacial deposits (e.g. Hu et al. 2015).

We further evaluate the reliability of the fine quartz (4 - 11 μm) grain measurements by their recuperation and recycling ratios. The recuperation values of all the fine grain quartz aliquots are below 5% (Fig. S4). The recycling

ratios range from 0.82 to 1.2, with 9 of the 12 fine grain quartz aliquots having recycling ratios within the acceptable range of 0.9 to 1.1. Only the aliquots with recycling ratios within the acceptable range were used for further analysis. Among these, one additional aliquot was also excluded because its D_e value fell outside 2σ of the distribution (Fig. 3). In the end, 8 fine grain quartz aliquots were used for OSL age calculation, resulting in an

5   average equivalent dose (D_e) of 178 ± 9 Gy (Table 1).

Annual dose rate (D) can be estimated from the U, Th and K concentrations, water contents and cosmic ray contribution (Guérin et al., 2011). An alpha efficiency factor (a-value) of 0.04 ± 0.02 for quartz (Rees-Jones, 1995) was used to calculate the alpha contribution to the total dose rate. The cosmic dose rate is negligible because the sediments are covered by thick ice and multiple dust layers, hence largely insulated from light and cosmic rays.

10   There are potentially two additional sources of radiation that are not included in the dose rate calculation: (1) radiation from the bedrock or subglacial sediment, and (2) radiation from dust layers in the core. Willerslev et al. (2007) suggested that the dose rate contribution from the underlying bedrock at the Greenland Dye 3 ice core drilling site was negligible following calculations based on radiation transport modelling software (MCNP5). Because no literature values are available to calculate the dose rate contribution from the underlying bedrock at our

15   drilling site, at the first stage we assume that its contribution to the dose rate was insignificant. As to radiation from dust layers in the core, we have not measured the dust concentrations of our Chongce ice cores, but A 18.7 m ice core drilled at the summit (6530 m a.s.l.) of the Chongce ice cap in 1992 gives a maximum dust mass concentration of 955 mg.kg^{-1} (Li et al., 2006). This provides a general impression of dust layers along the Chongce ice cores, which is ~3 orders of magnitude lower than the bottom sediment, suggesting insignificant influence of radiation

20   from dust layers in the core, given a similar radiation intensity of the dust layers in the core and the bottom sediment. Therefore, slightly increased dose rate would be expected if these additional sources of radiation were included, thus resulting in a slightly younger age.

The converted U, Th and K concentrations from the gamma measurements are close to the NAA results (Table 1), affirming the accuracy our element measurements. Water, if present in the sediment matrix, absorbs radiation

25   differently from mineral sediment, and has to be accounted for in the dose rate calculations. Since we have, for the moment, no information about the influence of the ice matrix on the dose rate, we use two extreme cases as our bounding scenarios, i.e., no water under the frozen condition and 30% water content if the sediment is saturated with water. The latter case (with high water content) results in a lower dose rate, hence an older age (Table 1).

The dated fine grain quartz aliquots are a mixture of eolian quartz and subglacially scoured quartz. But because the

30   distance from the summit of the Chongce ice cap to the drilling site is only several kilometers, and the ice cap is much shallower in comparison to the ice sheets, the scoured sediment experienced weak grinding. This suggests that even some of the fine grain quartz is derived from subglacial erosion, its portion might be very small. Thus the

dated aliquots are mostly an eolian origin, implying that the luminescence dating would represent the time for the ice to move from the surface to the bed

Our new data does not imply for an ice-free region in the Chongce region since 42 ± 4 ka ago, but for an ice-free condition below the elevation of the bottom at the drilling site during a (or more) warm period (or periods) since

5   this upper limit age (e.g., Marine Isotope Stage (MIS) 3, the Bølling-Allerød period, Holocene Climate Optimum). Takeuchi et al. (2014) reported radiocarbon dating of organic soil from the bottom of an 86.87 m ice core drilled at the top of the Grigoriev Ice Cap (41°58'33" N, 77°54'48" E) in the Tien Shan Mountains, showing that the age of the soil is 12 656 - 12 434 cal years before present. Takeuchi et al. (2014) suggested that the Grigoriev Ice Cap did not exist in the Bølling-Allerød period.

10   Given the surface elevation of the Chongce drilling site of 6100 m a.s.l. and the ice core length of 216.6 m, the elevation at the bottom of the Chongce drilling site is 5883.4 m a.s.l.. As to the Guliya ice core drilling site, its surface elevation of 6200 m a.s.l. and its length of 308.6 m result in an elevation at the bottom to be 5891.4 m a.s.l., suggesting that the age of the bottom ice at the Chongce and the Guliya drilling sites might be comparable. Thus our new data can not support the previously suggested age of more than 500 ka old of the Guliya bottom ice

15   (Thompson et al., 1997).

5 Conclusions

We provide an OSL age estimate of the basal sediment sample from the Chongce ice cap in the west Kunlun Mountains on the northwest TP, which gives an upper limit age of 42 ± 4 ka. The age is more than one order of magnitude younger than the previously suggested age of bottom ice in the west Kunlun Mountains. The major

20   limitation of the current work is the very small number of absolute datings and simple assumptions, but this preliminary work provides potential implications for exploring age of mountainous glacier bottom ice. Future work should include collecting more glacier basal sediment samples for the luminescence dating, and better understanding the unique processes for preserving the luminescence signal in the glacier basal sediment.

Author contribution

25   Shugui Hou designed this work and drilled the ice cores. Zhu Zhang and Shuangwen Yi performed the measurements. Shugui Hou wrote the draft of the paper. All authors contributed to discussion of the results.

Competing interests

The authors declare that they have no conflict of interest.

Acknowledgments

References

Banerjee, D., Murray, A. S., Bøtter-Jensen, L., and Lang, A.: Equivalent dose estimation using a single aliquot of polymineral fine grains, Radiat. Meas., 33, 73–94, 2001.

Bøtter-Jensen, L.,Thomsen, K. J., and Jain, M.: Review of optically stimulated luminescence (OSL) instrumental developments for retrospective dosimetry, Radiat. Meas., 45, 253–257, 2010.

Cheng, H., Zhang, P. Z., Spötl, C., Edwards, R. L., Cai, Y. J., Zhang, D. Z., Sang, W. C., Tan, M., and An, Z. S.: The climatic cyclicity in semiarid-arid central Asia over the past 500,000 years, Geophys. Res. Lett., 39, L01705, doi:10.1029/2011GL050202, 2012.

Cunningham, A.C. and Wallinga, J.: Selection of integration time intervals for quartz OSL decay curves, Quat. Geochron., 5, 657-666, 2010.

Duller, G.A.T.: Distinguishing quartz and feldspar in single grain luminescence measurements, Radiat. Meas., 37, 161–165, 2003.

Duller, G. A. T.: The Analyst software package for luminescence data: overview and recent improvements, Anc. TL, 33, 35-42, 2015.

Fuchs, M. and Owen, L. A.: Luminescence dating of glacial and associated sediments: review, recommendations and future directions, Boreas, 37, 636-659, doi:10.1111/j.1502-3885.2008.00052.x, 2008.

Guérin, G., Mercier, N., and Adamiec, G.: Dose rate conversion factors: update. Anc. TL, 29, 5–8, 2011.

Hu, G., Yi, C. L., Zhang, J. F., Liu, J. H., and Jiang, T.: Luminescence dating of glacial deposits near the eastern Himalayan syntaxis using different grain-size fractions, Quat. Sci. Rev., 124, 124-144, doi: 10.1016/j.quascirev.2015.07.018, 2015.

Li, Y., Yang, Y., Han, J., Xie, Z., Nakawo, M., and Goto-Azuma, K.: Persistent decrease of dust burden for about 100 years over middle-upper Troposphere of the southern Taklimakan Desert, China, J. Glaciol. Geocryol., 28, 873-878, 2006. (in Chinese with English abstract).

Murray, A.S., Marten, R., Johnston, A., and Martin, P.: Analysis for naturally occurring radionuclides at environmental concentrations by gamma spectrometry, J. Rad. Nuc. Chem., 115, 263-288, 1987.

Murray, A. S. and Wintle, A. G.: Luminescence dating of quartz using an improved single-aliquot regenerative-dose protocol, Radiat. Meas., 32, 57-73, doi: 10.1016/S1350-4487(99)00253-X, 2000.

Ou, X. J., Lai, Z. P., Zhou, S. Z., and Zeng, L. H.: Timing of glacier fluctuations and trigger mechanisms in eastern Qinghai–Tibetan Plateau during the late Quaternary, Quat. Res., 81, 464-475, doi:

5   10.1016/j.yqres.2013.09.007, 2014.

Owen, L. A., Spencer, J. Q., Ma, H., Barnard, P. L., Derbyshire, E., Finkel, R. C., Caffee, M. W., and Zeng, Y.N.: Timing of late quaternary glaciation along the southwestern slopes of the Qilian Shan, Tibet, Boreas, 32, 281–291, doi: 10.1111/j.1502-3885.2003.tb01083.x, 2003.

Rees-Jones, J.: Optical dating of young sediments using fine-grain quartz, Anc. TL 13, 9-14, 1995.

10   Takeuchi, N., Fujita, K., Aizen, V. B., Narama, C., Yokoyama, Y., Okamoto, S., Naoki, K., and Kubota, J.: The disappearance of glaciers in the Tien Shan Mountains in central Asia at the end of Pleistocene, Quat. Sci. Rev., 103, 26-33, doi: 10.1016/j.quascirev.2014.09.006, 2014.

Thompson, L. G., Yao, T., Davis, M. E., Henderson, K. A., Mosley-Thompson, E., Lin, P.-N., Beer, J., Synal, H.-A., Cole-Dai, J., and Bolzan, J. F.: Tropical climate instability: the last glacial cycle from a Qinghai-

15   Tibetan ice core, Science, 276, 1821-1825, doi: 10.1126/science.276.5320.1821, 1997.

Wang, L., Pan, G., Ding, J., and Yao, D.: Geological mapping of Qinghai–Tibet Plateau and its adjacent area (1: 1500000), Geological Publishing House, Beijing, 2013.

Willerslev, E., Cappellini, E., Boomsma, W., Nielsen, R., Hebsgaard, M. B., Brand, T. B., Hofreiter, M., Bunce, M., Poinar, H. N., Dahl-Jensen, D., Johnsen, S., Steffensen, J. P., Bennike, O., Schwenninger, J.-L., Nathan, R.,

20   Armitage, S., de Hoog, C.-J., Alfimov, V., Christl, M., Beer, J., Muscheler, R., Barker, J., Sharp, M., Penkman, K. E. H., Haile, J., Taberlet, P., Gilbert, M. T. P., Casoli, A., Campani, E., and Collins, M. J.: Ancient biomolecules from deep ice cores reveal a forested southern Greenland, Science, 317, 111-114, doi: 10.1126/science.1141758, 2007.
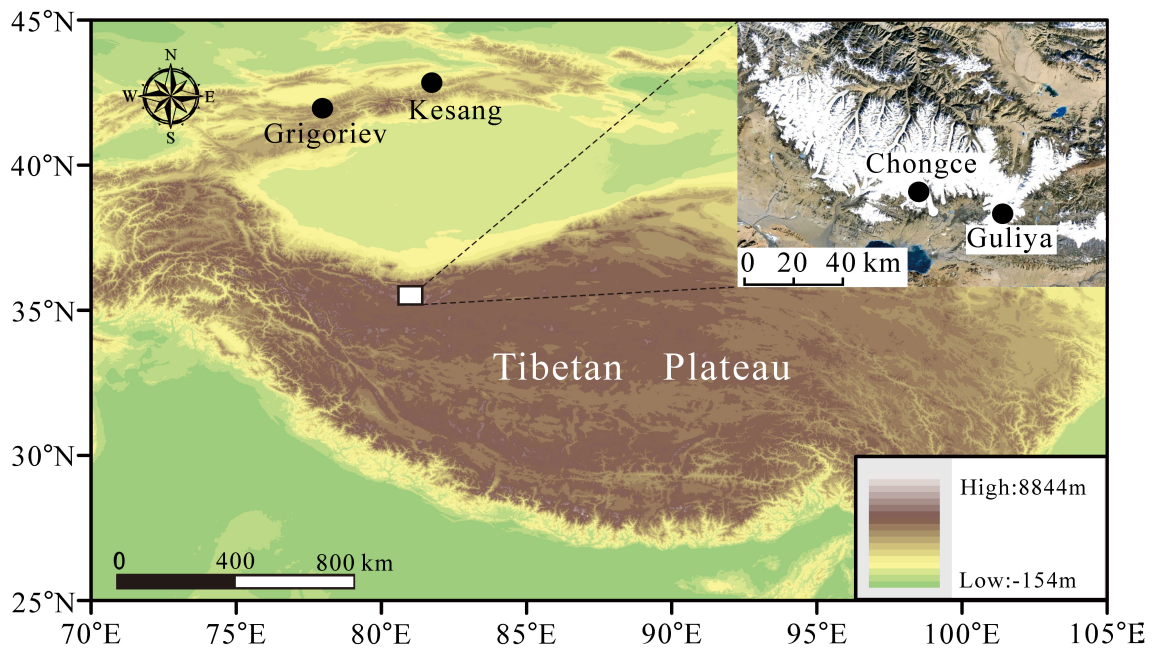
Figure 1: Study area map showing the locations of the Chongce and Guliya ice caps in the west Kunlun Mountains,

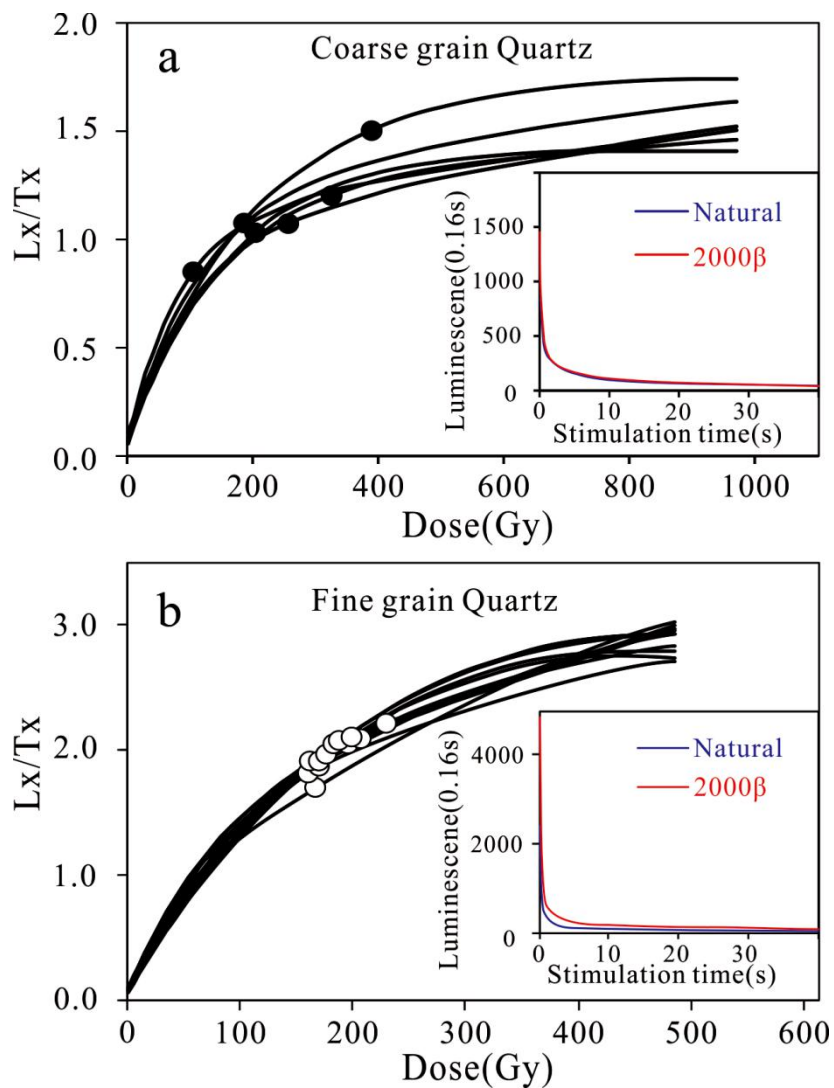the Kesang cave and the Grigoriev Ice Cap.

Figure 2: The OSL dose-response and decay curves of the coarse and fine grain quartz aliquots. Inserts show decay curves of the natural and regenerated dose (2000β) of the sample.
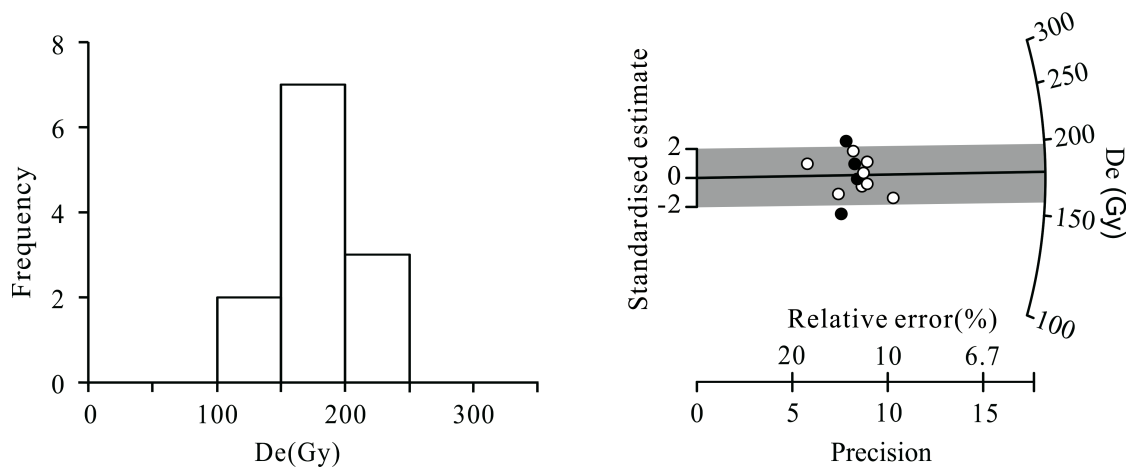
Figure 3: D$_e$ distribution histogram (left) and radial plot (right) showing the distribution of D$_e$ results for the fine grains. The shaded region represents 2σ width of the distribution. The filled symbol represents the aliquots that were excluded in the final age calculation.

Table 1. Results of the fine quartz grains with their corresponding OSL ages.

Sample	U (ppm)		Th (ppm)		K (%)		D$_e$	Water content	Dose rate	Age
	Gamma	NAA	Gamma	NAA	Gamma	NAA	(Gy)	(%)	(Gy/ka)	(ka)
CCICE	3.66 ± 0.15	3.45 ± 0.12	11.21 ± 0.42	11.40 ± 0.32	3.52 ± 0.10	3.48 ± 0.08	178 ± 9	0	5.81 ± 0.46	31 ± 3
								30 ± 15	4.24 ± 0.37	42 ± 4

11